Journal of Chemical Technology and Metallurgy, 61, 2, 2026, 293-301

STRUCTURE AND OPTICAL CHARACTERISTICS OF GLASSES IN THE TeO_2-BaO-Bi_2O_3-B_2O_3 SYSTEM

T. Tasheva

Department of Silicate Technology
University of Chemical Technology and Metallurgy,
8 Kliment Ohridski Blvd., Sofia 1797, Bulgaria
E-mail: tina.tasheva@uctm.edu (T.T.)

Received 09 August 2025
Accepted 03 September 2025
DOI: 10.59957/jctm.v61.i2.2026.10

ABSTRACT

A series of glasses in the BaO-TeO_2-Bi_2O_3-B_2O_3 system, was prepared by melt quenching technique. The amorphous nature of the obtained glasses was confirmed by X-ray powder diffraction analysis. The experimental densities were found to be in the range 5.170 to 5.831 g cm^{-3}. Key structural parameters, including molar volume, oxygen packing density, optical basicity, interionic interaction parameter, and single bond strength, were evaluated to understand the compositional effects on the glass network. Structural characterization using infrared and Raman spectroscopy further elucidated the bonding and vibrational features of the glasses. The refractive indices were measured experimentally and compared with theoretical values calculated using the polarization approach, revealing a strong correlation between experimental and theoretical results.

Keywords: *Borate glasses, Refractive index, IR spectroscopy, Raman spectroscopy.*

INTRODUCTION

The structure of oxide glasses is strongly influenced by the way different network-forming and modifying oxides share and rearrange their oxygen environments. In compositions built from TeO_2, B_2O_3, Bi_2O_3 and BaO, each oxide plays a distinct role and contributes differently to the final structural arrangement.

Tellurite glasses based on TeO_2 are characterized by a network built mainly from TeO_4 trigonal bipyramids together with smaller fractions of TeO_3 trigonal pyramids [1 - 3]. The TeO_4 groups act as the network former of the structure by linking through shared oxygen corners. In contrast, the TeO_3 units usually arise when modifiers are added or when non-bridging oxygens are formed. The ease with which the glass network shifts between these coordination states contributes to several typical features of tellurite materials, including their low phonon energies, high refractive index, and broad infrared transparency. The lone-pair electrons associated with Te^{4+} ions further influence the network by creating asymmetry and enhancing the overall polarizability [3]. Based on the group optical basicity introduced by Duffy and Ingram [4], Dimitrov and Komatsu [3, 5] extended the concept to describe the optical basicity of individual TeO_n units in tellurite glasses. Their analysis of various binary and ternary tellurite systems showed that TeO_4 unit with one non-bridging oxygen (λTeO_{4-} = 1.23), TeO_4 unit without nonbridging oxygen (λTeO_{4° = 0.99), and terminal TeO_3 unit with two non-bridging oxygens (λTeO_{3-} = 0.82). Consequently, TeO_4 trigonal-bipyramidal units that are distorted through the presence of non-bridging oxygens and unequal Te-O bond lengths are expected to enhance the electronic polarizability [3, 5].

Bismuth oxide, with its heavy and highly polarizable cations, usually increases the overall compactness of the network and can introduce different Bi-O coordination units [6, 7]. Bismuth-containing glasses are known for their distinctive optical behaviour, largely attributed to the high atomic weight and strong electronic polarizability of Bi^{3+} ions [6]. These properties

contribute to the high refractive index often observed in Bi_2O_3-rich compositions, making them attractive for various photonic applications. Structurally, Bi_2O_3 can act either as a network former or as a modifier, commonly giving rise to BiO_6 polyhedra. The incorporation of such units tends to loosen the glass network by lowering its connectivity and increasing the number of non-bridging oxygens, a trend that is reflected in characteristic changes in their spectra. This structural depolymerization is typically accompanied by a decrease in the optical band gap, which broadens the material's absorption into the visible and near-infrared regions. The addition of Bi_2O_3 also lowers the phonon energy of the glass, enhancing its infrared transmission-an important advantage for mid-IR lasers and photonic devices. Furthermore, the stereochemically active lone-pair electrons associated with Bi^{3+} can strengthen the nonlinear optical response [6].

Borate glasses enriched with large amounts of heavy-metal oxides tend to exhibit high densities, making them good candidates for radiation-shielding applications. At the same time, incorporating significant concentrations of optically active ions into B_2O_3-based networks opens opportunities for developing various photonic components [7]. B_2O_3 is a well-known glass former, and borate glasses have been widely investigated because of their interesting properties. In these materials, the proportion of BO_4 to BO_3 units depends on the type and amount of modifier added. When network modifiers are introduced, borate properties often show maxima or minima at certain modifier concentrations-an effect called the borate (or boron oxide) anomaly. At low modifier levels, the modifier mainly converts trigonal $BØ_3$ units into tetrahedral $BØ_4$- units, rather than immediately generating nonbridging oxygens (NBOs), which generally form only at higher modifier contents. Borate units are typically described as B(n), where "n" represents the number of bridging oxygen atoms (Ø) linking each unit to its neighbours [7, 8].

Thus, the structural behaviour of glasses in the TeO_2-B_2O_3-Bi_2O_3-BaO system results from the combined influence of their network-forming and modifying oxides, each contributing distinct coordination units and oxygen environments. TeO_2 forms a flexible tellurite network whose shift between TeO_4 and TeO_3 units enhances polarizability and infrared transparency. Bi_2O_3 introduces highly polarizable Bi-O units that depolymerize the network, increase refractive index, and lower phonon energy. B_2O_3 contributes its BO_3/BO_4 structural units, whose distribution depends strongly on modifier content and gives rise to the well-known borate anomaly. Together, these oxides create a structurally versatile glass matrix with tunable optical, vibrational, and electronic properties suitable for photonic and radiation-related applications.

This study aims to investigate the mutual influence of TeO_2, B_2O_3, Bi_2O_3, and BaO on the structure, and to investigate how the main structural units affect the resulting optical and physical properties of the glasses.

EXPERIMENTAL

The following compositions $xBaO.TeO_2.(60\text{-}2x)Bi_2O_3.40B_2O_3$, where x = 0, 5, 10, 15, and 20 mol %, were prepared by melt-quenching technique. The raw materials TeO_2 (Alfa Aesar, Thermo Scientific, ThermoFisher, Kandel, Germany; 99.99 %), Bi_2O_3 (Acros Organics BV, Thermo Fisher Scientific, Geel, Belgium; 99.7 %), $BaCO_3$ (Alfa Aesar), and B_2O_3 (Alfa Aesar, 99 %) were first mixed thoroughly in an agate mortar. The homogenized mixtures were then heated up to 650°C for 20 min and then heated at 1000°C for 20 min in an electric furnace, followed by melt quenching. The XRD analysis were performed using Empyrean (Malvern-Panalytical) diffractometer, CuKα radiation at 40 kV and 30 mA for the samples in the range of 5.3 to 80° 2θ, with a constant step size of 0.03° 2θ and a counting time of 52.5 sec per step. The glass densities were determined following the Archimedes principle using a Mettler Toledo New Classic ME 104 analytical balance (Mettler Toledo, Greifensee, Switzerland), equipped with a solid-sample density measurement kit and distilled water as the immersion medium. For each composition, at least ten measurements were performed on no fewer than three different samples. From the experimentally evaluated density values, the molar volume (V_m) is estimated, by Eq. (1):

$$V_m = \frac{\sum x_i M_i}{d_i}, \quad (1)$$

where x_i is the molar fraction of each component i, M_i is the molecular weight, d_i is the glass density [9]. The oxygen packing density (OPD) of the glasses was also estimated using the following Eq. (2),

$$OPD = 1000.N_O^{2-}.\frac{d_i}{M_i}, \quad (2)$$

where N_O^{2-} is the number of oxygens per formula unit [9].

The infrared spectra were collected using a Varian 600-IR FT-IR spectrometer (Melbourne, Australia) over the range 4000 - 400 cm^{-1}, with samples prepared as KBr pellets. The absorption-band positions have an accuracy of ± 3 cm^{-1}. Raman spectra were obtained using a Renishaw inVia Raman microscope (Gloucestershire, UK) equipped with a Leica DM2700 M microscope (Leica Microsystems CMS GmbH, Wetzlar, Germany). Excitation was provided by a 633 nm He-Ne laser, with the power reduced to 3.2 mW to prevent local heating. A 50× objective lens was used to focus the laser and collect the backscattered signal. The illuminated spot on the sample surface was approximately 3 μm in diameter. Spectra were recorded in the 90 - 1280 cm^{-1} range, with a wavenumber accuracy of 1 cm^{-1}. The refractive index of light was measured by Woollam M2000D ellipsometer in the range of 193 nm to 1000 nm. The data collection and analysis software is CompleteEASE 5.10 J. A. Woollam Co., Inc.

RESULTS AND DISCUSSION

The compositions of the obtained samples are presented in Table 1. The presence of an amorphous halo confirms the amorphous nature of the obtained samples by powder X-ray analysis (Fig. 1). The obtained results for density, molar volume, and oxygen packing density (OPD) clearly demonstrate the influence of chemical composition on the structure of glasses in the TeO_2-B_2O_3-Bi_2O_3-BaO system (Table 1). The lowest value of the density is recorded for sample A3, which contains 20 mol % BaO together with moderate amounts of TeO_2 and Bi_2O_3. In this composition, Ba^{2+} ions disrupt the Te-O and B-O network, producing a more open structure. Despite the lower density, A3 has the lowest molar volume and the highest OPD value. This combination suggests that the breakdown of network connectivity leads to the formation of additional non-bridging oxygens and to a rearrangement of the oxygen units into locally compact groupings, even if the overall structure becomes less tightly packed. A different picture is seen in sample A5, which also contains 20 mol % BaO but completely lacks TeO_2. Its high Bi_2O_3 content (40 mol %) compensates for the network-modifying action of BaO and results in a much higher density. Bi_2O_3 is known to contribute significantly to mass and to participate in the network through different structural units, such as BiO_6 octahedra and BiO_3 pyramids. The presence of these units helps to stabilise the medium-range structure and counteracts the expansion that BaO would otherwise introduce. The BaO-free glass (A4) provides a useful reference point. With both TeO_2 and Bi_2O_3 present at 20 - 40 mol %, A4 exhibits a dense and relatively compact network. TeO_2 could enhance the degree of polymerization through TeO_4 and TeO_{3+1} units, which contribute to the formation of a more rigid three-dimensional structure. Its OPD value is moderate, reflecting a balance between the heavy, polarizable Bi-O units and the more tightly connected Te-O network. The intermediate compositions (A1 and A2) fall between these two extremes. Increasing the BaO content from 10 % to 15 % leads to a gradual decrease in density and a slight reduction in molar volume, consistent with partial network disruption. The OPD values of both samples show that, while the structure becomes more

Table 1. Compositions, molar mass, M, density, d, molar volume, V_m, molar refraction, R_m, oxygen packing density, OPD.

	Compositions, mol %				M,	d,	V_m,	R_m,	OPD,
	BaO	TeO_2	B_2O_3	Bi_2O_3	g mol^{-1}	g cm^{-3}	cm^3 mol^{-1}	cm^3 mol^{-1}	mol cm^{-3}
A4	-	20	40	40	246.152	5.583	44.09	18.26	63.51
A1	10	10	40	40	245.525	5.552	44.22	17.79	61.05
A2	15	15	40	30	214.575	5.411	39.66	16.22	64.30
A3	20	20	40	20	183.626	5.170	35.52	14.69	67.57
A5	20	-	40	40	244.897	5.831	42.00	17.32	61.91

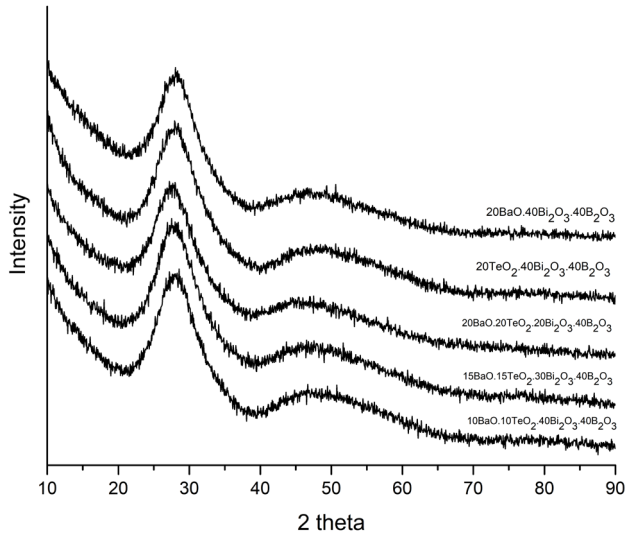

Fig. 1. XRD patterns of the samples.

modified, the presence of Bi_2O_3 still ensures a degree of compactness in the oxygen arrangement. These results illustrate two key points. First, Bi_2O_3 influences the density and medium-range order of the glasses and can even dominate the structural response when present in high concentrations. Second, BaO acts as an effective modifier, increasing the density and altering the oxygen topology, but its impact also depends on the Bi_2O_3 and TeO_2 amount.

The structure of the obtained glasses was investigated using FT-IR and Raman spectroscopy (Figs. 2 and 3). The FT-IR spectra are characterized by three well defined regions: above 1200 cm^{-1}, around 900 cm^{-1} and around 680 cm^{-1} (Fig. 2). All samples exhibit the characteristic vibrational features of mixed tellurite-borate glass networks, yet the positions and intensities of the absorption bands vary systematically with composition, indicating structural rearrangements within the glass matrix.

The high-frequency region contains two partially overlapping bands located near 1310 - 1300 cm^{-1} and 1270 - 1220 cm^{-1}. These absorptions could be attributed to the asymmetric stretching vibrations, $\nu_d^{as}(E)$, of B-O bonds in trigonal BO_3 units. [7, 8]. Their gradual shifts with composition suggest changes in the relative populations of BO_4 and BO_3 structural units. The peaks in the high frequency region shift toward lower wavenumbers with increasing Bi_2O_3 or BaO content. This behaviour reflects an enhanced degree of network modification and the formation of non-bridging oxygens.

The broad absorptions observed in the 968 - 896 cm^{-1} interval originate from the stretching vibrations of Te-O_{ax} and Te-O_{eq} bonds in both TeO_4 and distorted TeO_3 units, as well as B-Ø ring and B-O terminal stretch in $[B_3O_9]^{9-}$ rings of $B\O_2O_2^{3-}$ tetrahedral units B-Ø stretch in $B\O_4$ units [7 - 11]. The band at 685 cm^{-1} could be assigned to the degenerate stretching vibrations $\nu_d^{as}TeO_3$ of TeO_3 trigonal pyramids and a total decrease of the tellurite units, while the band at 697 cm^{-1} could be due to the out-of-plane bend of triangular borate units [9, 11].

At the lower frequency region, a distinct band located around 464 cm^{-1} is assigned to bending vibrations of Te-O-Te bridges, in addition to deformation modes involving Bi-O bonds [7, 9]. The increasing intensity of this band in Bi_2O_3-rich samples is consistent with the high polarizability and structural contribution of Bi-O units to the glass network [6, 7]. Overall, the FT-IR results confirm that the incorporation of Bi_2O_3 and BaO significantly influences the connectivity of the Te-O and B-O sub-networks. Increasing the modifier content promotes depolymerization of the glass network, leading to a higher concentration of TeO_3 units and non-bridging oxygens. These structural changes are reflected consistently across all spectral regions.

Fig. 3 displays the Raman spectra of the glasses. In the low-frequency region below 250 cm^{-1}, all samples show strong bands near 141 - 148 cm^{-1}. These modes are typically assigned to bending vibrations and lattice-

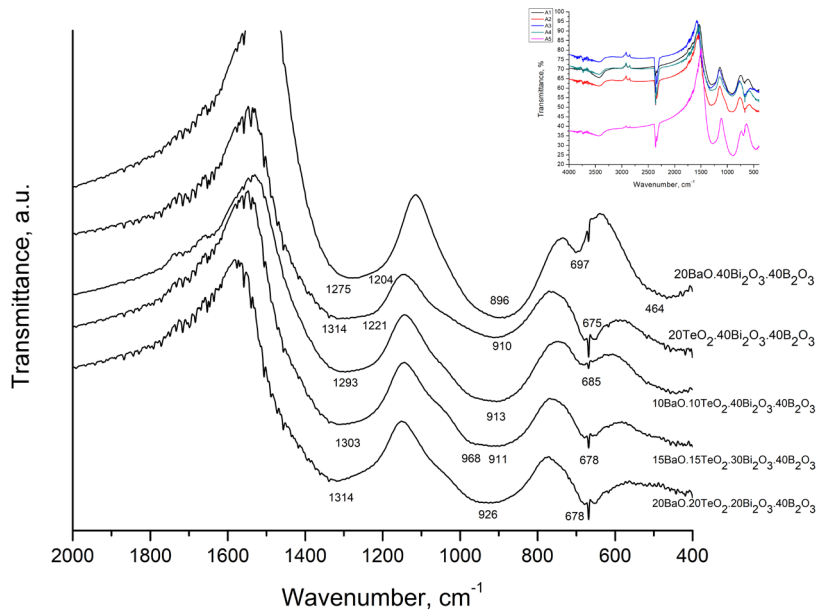

Fig. 2. FT-IR spectra of the samples.

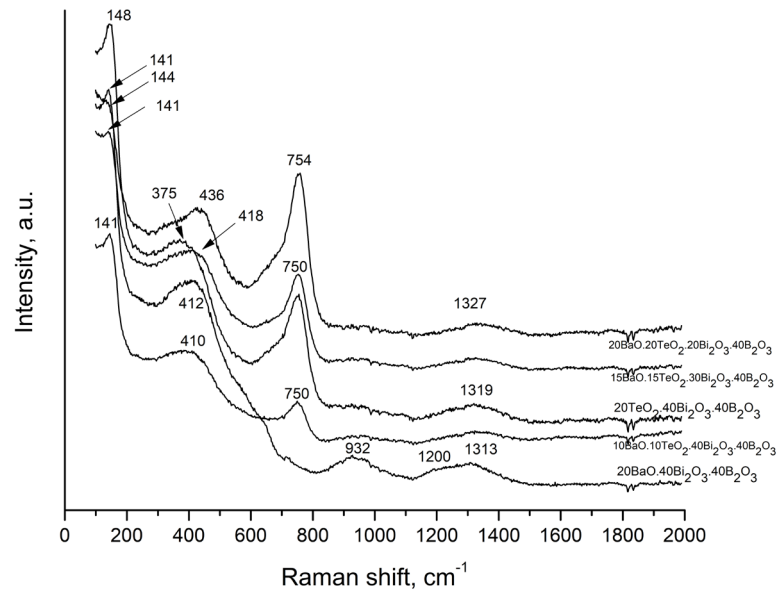

Fig. 3. Raman spectra of the samples.

type motions involving heavy-metal cations, particularly Bi-O [7, 10]. $Bi_3B_5O_{12}$ shows a low-frequency vibration near 148 cm^{-1}, while $Bi_4B_2O_9$ exhibits a similar band around 140 cm^{-1}. In both compounds, the oxygen atoms are coordinated exclusively to bismuth polyhedra-often referred to "free" O^{2-} ions [7]. The presence and the relatively high intensity of these bands reflect the significant contribution of highly polarizable Bi^{3+} ions to the glass network.

The region between 350 and 450 cm^{-1} contains several distinct bands centered around 375, 410 - 418, and 436 cm^{-1}. These vibrations correspond to bending vibrations of TeO_4 trigonal bipyramids and TeO_{3+1}/TeO_3 units, as well as deformation of B-O-B linkages within the borate sub-network [9 - 11]. The gradual intensity redistribution in this region with changing composition

suggests increased distortion of the tellurite units and a shift toward less symmetrical TeO_3 species as modifier oxides are introduced.

A prominent high-intensity band appears in all samples containing TeO_2 at about 750 - 754 cm^{-1} and increases its intensity with increasing TeO_2 content. This peak is characteristic of the symmetric stretching vibrations of Te-O bonds in TeO_{3+1} structural units and is widely regarded as a fingerprint feature of tellurite glasses [10]. Band at 670 cm^{-1} is characteristic for the presence of TeO_4 structural units, and 762 cm^{-1} is typical for the TeO_3^{2-} [10]. Such bands in our Raman spectra are not observed.

In the intermediate region between 900 and 1200 cm^{-1}, weaker bands are observed at 932, 1200, and 1313 - 1327 cm^{-1}. These features are attributed to stretching vibrations of BO_4 tetrahedra and asymmetric stretching vibrations of BO_3 units. The broadening and slight shifts of these bands reflect the progressive modification of the borate network, including changes in the BO_3/BO_4 ratio induced by the introduction of Ba^{2+} and Bi^{3+} ions. The increasing contribution of Bi_2O_3 and BaO promotes the increase in the degree of disorder in the tellurite network and alters the coordination environment within the borate sub-network.

Both FT-IR and Raman analyses confirm that the structural evolution of the TeO_2-B_2O_3-Bi_2O_3-BaO glasses is governed by the mutual influence between glass-forming (B_2O_3), conditional glass-formers (TeO_2, Bi_2O_3) and network-modifying (BaO) oxides. Both vibrational spectra reveal the presence of more distorted TeO_3/TeO_{3+1} species and a modification of the borate sub-network, consistent with the depolymerization effects expected from increasing BaO content. These spectroscopic trends correlate well with the physical parameters. A decrease in density and molar volume in BaO-rich glasses (e.g., A3) reflects enhanced disruption of Te-O and B-O linkages, while the high OPD values demonstrate that network breakdown is accompanied by the formation of additional non-bridging oxygen units and localized oxygen compaction. In contrast, glasses rich in Bi_2O_3 (e.g., A5) show higher density and moderated OPD values, in agreement with the Raman/FT-IR evidence for stabilization of medium-range structure through Bi-containing structural units. Overall, the vibrational and physical property data collectively indicate that BaO promotes network modification and oxygen rearrangement, whereas Bi_2O_3 enhances rigidity and medium-range order. Their combined influence provides an effective means to tailor the structural packing and connectivity of the glasses.

Electronic polarizability is the most important component of polarizability when interpreting the optical properties of materials. The estimation of electronic polarizability is a subject of the polarizability approach. The polarizability approach is based on the Lorentz-Lorenz equation Eq. (3), which correlates the molar refraction R_m with the linear refractive index n_0 and the molar volume V_m of the material:

$$R_m = \frac{(n_0^2 - 1)}{(n_0^2 + 2)} V_m \quad (3)$$

Dimitrov and Sakka further expanded this method by calculating the oxide-ion polarizability $\alpha_{O^{2-}}(n_0)$ and the optical basicity $\Lambda(n_0)$ for a variety of simple oxides using Eq. (4) and Eq. (5), [12]:

$$\alpha_{O^{2-}}(n_0) = \left[\frac{R_m}{2.52} - \sum \alpha_i\right](N_{O^{2-}})^{-1} \quad (4)$$

$$\Lambda(n_0) = 1.67\left(1 - \frac{1}{\alpha_{O^{2-}}}\right) \quad (5)$$

Further information about the chemical bonding in the glass matrix could be obtained by estimating the interaction parameter A, $Å^{-3}$ and the single bond strength B_{M-O}, kJ mol^{-1}. The interaction parameter, originally introduced by Yamashita and Kurosawa and later adapted for oxide glasses by Dimitrov and Komatsu, quantifies the overlap between the electron clouds of cations and oxide ions and reflects the polarizability of the average oxide ion [13 - 16]. In this study the interaction parameter was calculated using equivalent oxide fractions X(BaO), $X(TeO_2)$, $X(Bi_2O_3)$, $X(B_2O_3)$, the oxide-ion polarizability $\alpha_{O^{2-}}$, and the cation polarizabilities $\alpha(Ba^{2+})$ = 1.595 $Å^3$, $\alpha(Te^{4+})$ = 1.595 $Å^3$, $\alpha(B^{3+})$ = 0.002 $Å^3$, and $\alpha(Bi^3)$ = 1.508 $Å^3$, with Pauling's value of 3.921 $Å^3$ for O^{2-} [17]. The oxide ion polarizability was calculated both theoretically and experimentally. Duffy and Ingram proposed that the theoretical optical basicity (Λ_{th}) of a glass can be estimated by considering the contributions of all constituent oxides, including those forming bridging or non-bridging oxygens [18, 19]. Although this approach does not account for changes in cation coordination, it still provides a useful indication of the expected overall optical basicity of a given composition.

The optical basicity values for the single oxides used are $\Lambda(BaO) = 1.21$, $\Lambda(TeO_2) = 1.05$, $\Lambda(Bi_2O_3) = 1.19$, and $\Lambda(B_2O_3) = 0.46$ [16, 20] calculated by Eq. (6):

$$\Lambda_{th} = X_{BaO}\Lambda_{BaO} + X_{TeO_2}\Lambda_{TeO_2} + X_{Bi_2O_3}\Lambda_{Bi_2O_3} + X_{B_2O_3}\Lambda_{B_2O_3} \quad (6)$$

where X_{BaO}, X_{TeO_2}, $X_{Bi_2O_3}$, and $X_{B_2O_3}$ are the equivalent fractions based on the amount of oxygen contributed by each oxide to the overall glass stoichiometry. The obtained results for the optical basicity, Λ, oxide ion polarizability $\alpha_{O^{2-}}$, Å^3, and interaction parameter are presented in Tables 2 and 3.

A comparison of the theoretical values (Table 2) and experimentally derived parameters (Table 3) provides important insight into the structural and electronic behaviour of the glasses. In general, the theoretical optical basicity (Λ_{th}) and the basicity derived from the refractive index ($\Lambda(n_0)$) follow the same compositional trend, although the experimental values are consistently higher. This systematic increase is expected, as $\Lambda(n_0)$ incorporates the real polarizability contributions of the cations, which are not considered in the theoretical values, thus tend to enhance the electron density available for optical interactions more strongly than predicted by purely additive theoretical models. A similar relationship is observed in the oxide ion polarizability. The values obtained theoretically ($\alpha_{O^{2-}}$) and experimentally ($\alpha_{O^{2-}}(n_0)$) both decrease with increasing BaO content in glasses containing moderate Bi_2O_3 (A1 - A3). This behaviour reflects the reduction of highly polarizable Te-O units as Ba^{2+} modifies the network. However, the experimentally derived $\alpha_{O^{2-}}(n_0)$ values are consistently larger than their theoretical counterparts, confirming that the presence of Bi-O structural units significantly enhances the real electronic polarizability beyond simple compositional predictions.

The interaction parameter A shows good qualitative agreement between theory and experiment. For samples A1 - A3, both A_{th} and $A(n_0)$ increase slightly with BaO content, indicating enhanced ion-oxygen interactions as the network becomes more depolymerized. Quantitatively, however, the experimental $A(n_0)$ values are higher, which again reflects the stronger-than-expected contribution of Bi^{3+} to the electronic environment. Sample A4 (BaO-free) shows the highest theoretical value of A_{th}, consistent with a more polymerized Te-O/B-O network, while its experimental value is markedly lower due to the possible stabilizing and polarizable effects of Bi_2O_3 observed in refractive index measurements.

Table 2. Compositions, mol %, theoretical optical basicity, Λ_{th}, oxide ion polarizability $\alpha_{O^{2-}}$, Å^3, interaction parameter A, Å^{-3}, single bond strength, B_{M-O}, kJ mol^{-1}.

	BaO	TeO_2	B_2O_3	Bi_2O_3	Λ_{th}	$\alpha_{o^{2-}}$, Å^3	A_{th}, Å^{-3}	$n_{0(th)}$	B_{M-O}, kJ mol^{-1}
A4	-	20	40	40	0.857	2.054	0.077	1.792	297
A1	10	10	40	40	0.856	2.051	0.078	1.758	283
A2	15	15	40	30	0.831	1.991	0.085	1.778	294
A3	20	20	40	20	0.803	1.927	0.092	1.793	304
A5	20	-	40	40	0.855	2.048	0.080	1.779	268

Table 3. Compositions, mol %, experimental refractive index, n_0, optical basicity based on the refractive index $\Lambda(n_0)$, the oxide ion polarizability based on refractive index $\alpha_{O^{2-}}(n_0)$, Å^3, interaction parameter based on refractive index $A(n_0)$, Å^{-3}.

	BaO	TeO_2	B_2O_3	Bi_2O_3	n_0, exp (589 nm)	$\Lambda(n_0)$	$\alpha_{o^{2-}}$, Å^3	$A(n_0)$, Å^{-3}
A4	-	20	40	40	1.868	0.940	2.289	0.061
A1	10	10	40	40	-	-	-	-
A2	15	15	40	30	1.698	0.761	1.837	0.098
A3	20	20	40	20	1.782	0.814	1.951	0.090
A5	20	-	40	40	1.902	0.974	2.400	0.056

Chemical bonding was also assessed through the average single-bond strength, following Sun's dissociation-energy concept and its adaptation to glasses by Dimitrov and Komatsu [21, 22]. The following values of the single bond strengths of M-O in the corresponding individual oxide B_{Ba-O} = 138 kJ mol^{-1}, B_{Te-O} = 285 kJ mol^{-1}, B_{B-O} = 498 kJ mol^{-1}, and B_{Bi-O} = 102.5 kJ mol^{-1} were used [6, 17]:

$$B_{M-O} = a.B_{Ba-O} + b.B_{Te-O} + c.B_{B-O} + d.B_{Bi-O}, \text{ kJ mol}^{-1} \quad (7)$$

where a, b, c, and d are the mole fractions of the oxides.

The results of the single bond strength of the glasses are presented in Table 2. The studied glasses exhibit low average bond strengths (283 - 304 kJ mol^{-1}), indicating weak interionic interactions and relatively weak M-O bonds. The single bond strength B_{M-O} shows an inverse relationship with polarizability, as expected. The BaO-rich samples (e.g., A3) show reduced B_{M-O}, which correlates with their higher polarizability and increased network modification. Experimentally, this trend is confirmed through lower refractive index-derived interaction parameters.

In summary, the comparison shows that the experimental optical parameters consistently exceed their theoretical values, reflecting the significant influence of Bi-O units and the real structural rearrangements detected by refractive index measurements. Both theoretical and experimental analyses reveal the same compositional trends, confirming that BaO acts as a network modifier that reduces bond strength and increases electronic polarizability, whereas Bi_2O_3 and TeO_2 enhance medium-range structural stability and contribute strongly to optical basicity. This agreement demonstrates that theoretical models describe the glass system well but underestimate the electronic contribution of heavy-metal oxide structural units.

CONCLUSIONS

Glasses in the TeO_2-BaO-Bi_2O_3-B_2O_3 system were successfully synthesized, and their structural, physical, and optical properties were systematically evaluated. The combined FT-IR and Raman analyses confirmed the coexistence and evolution of the structural units, demonstrating that BaO acts as a strong network modifier, while Bi_2O_3 contributes both to network depolymerization and to enhanced electronic polarizability. Density, molar volume, and oxygen packing density trends revealed that increasing BaO reduces network connectivity, whereas higher Bi_2O_3 stabilizes the medium-range structure due to the heavy and highly polarizable Bi^{3+} cations. Theoretical optical basicity and oxide ion polarizability values showed good agreement with experimentally derived parameters, confirming the sensitivity of the Polarizability approach for evaluating electronic polarizability within multicomponent oxide systems. The glasses exhibit high refractive index values, primarily influenced by the presence of Bi_2O_3 and TeO_2. Overall, the results demonstrate that the mutual influence between TeO_2, BaO, Bi_2O_3, and B_2O_3 enables fine structural and optical tunability. The strong correlation between network structure, polarizability, and refractive index highlights the potential of these glasses for photonic, infrared-optical, and radiation-related applications.

Acknowledgements

This study is funded by the National Science Fund, Contract. No KP-06-H78/4 of 05.12.2023, topic: "Study of the influence of submicrostructure on the optical and dielectric characteristics of oxide glasses and glass-ceramics with high oxygen polarizability".

Authors' contributions

T.T.: Conceptualisation, Methodology, Investigation, Writing - original draft preparation, Writing - review and editing.

REFERENCES

1. M. Arnaudov, V. Dimitrov, Y. Dimitriev, L. Markova, Infrared-spectral investigations of tellurites, Mat. Res. Bull., 17, 1982, 1121-1129.
2. Y. Dimitriev, V. Dimitrov, M. Arnaudov, IR spectra and structures of tellurite glasses, J. Mat. Sci., 18, 1983, 1353-1358.
3. T. Komatsu, V. Dimitrov, Features of electronic polarizability and approach to unique properties of tellurite glasses, Int. J. Appl. Glass Sci., 00, 2019, 1-19.
4. J.A. Duffy, M.D. Ingram, An interpretation of glass chemistry in terms of the optical basicity concept, J. Non-Cryst. Solids, 21, 1976, 373-410.

5. V. Dimitrov, T. Komatsu, Group optical basicity of tellurite glasses, Phys. Chem. Glasses Eur. J. Glass Sci. Technol. B, 52, 2011, 138-141.
6. T. Komatsu, V. Dimitrov, T. Tasheva, T. Honma, A Review: A New Insight for Electronic Polarizability and Chemical Bond Strength in Bi_2O_3-Based Glasses, J. Non-Cryst. Solids, 550, 2020, 120365.
7. B. Topper, E.M. Tsekrekas, L. Greiner, R.E. Youngman, E.I. Kamitsos, D. Möncke, The dual role of bismuth in Li_2O-Bi_2O_3-B_2O_3 glasses along the orthoborate join, J. Am. Ceram. Soc., 105, 2022, 7302-7320. https://doi.org/10.1111/jace.18699.
8. T. Tasheva, G. Valova, FT-IR and Raman spectroscopy of ZnO and MgO containing glasses in the B_2O_3/Na_2O/CaO/P_2O_5 system, J. Chem. Technol. Metall., 59, 6, 2024, 1391-1398. DOI: 10.59957/jctm.v59.i6.2024.14
9. T. Tasheva, V. Dimitrov, Correlation between structure and optical basicity of glasses in the TeO_2-V_2O_5-MoO_3 system, J. Non-Cryst. Solids, 570, 2021, 120981. https://doi.org/10.1016/j.jnoncrysol.2021.120981
10. N.S. Tagiara, E. Moayedi, A. Kyritsis, L.Wondraczek, E.I. Kamitsos, Short-Range Structure, Thermal and Elastic Properties of Binary and Ternary Tellurite Glasses, J. Phys. Chem. B, 123, 2019, 7905-7918. DOI: 10.1021/acs.jpcb.9b04617
11. C.P.E. Varsamis, N. Makris, C. Valvi, E.I. Kamitsos, Short-range structure, the role of bismuth and property-structure correlations in bismuth borate glasses, Phys. Chem. Chem. Phys., 23, 16, 2021, 10006-20.
12. V. Dimitrov, S. Sakka, Electronic oxide polarizability and optical basicity of simple oxides. I, J. Appl. Phys., 79, 1996, 1736-1740.
13. J. Yamashita, T. Kurosawa, The theory of the dielectric constant of ionic crystals III, J. Phys. Soc. Jpn., 10, 1955, 610.
14. U.C. Dikshit, M. Kumar, Analysis of electronic polarizabilities in ionic crystals, Phys. Stat. Sol. B, 165, 1991, 599.
15. V. Dimitrov, T. Komatsu, Effect of interaction on the electronic polarizability, optical basicity and binding energy of simple oxides, J. Ceram Soc. Jpn., 107, 11, 1999, 1012-1018.
16. V. Dimitrov, T. Komatsu, Interionic interactions, electronic polarizability and optical basicity of oxide glasses, J. Ceram. Soc. Jpn., 108, 2000, 330.
17. V. Dimitrov, T. Komatsu, An interpretation of optical properties of oxides and oxide glasses in terms of the electronic ion polarizability and average single bond strength (Review), J. Univ. Chem. Technol. Metall., 45, 3, 2010, 219-250.
18. J.A. Duffy, M.D. Ingram, An interpretation of glass chemistry in terms of the optical basicity concept, J. Non-Cryst. Solids, 21, 1976, 373-410.
19. J. A. Duffy, M.D. Ingram, in Optical properties of glasses, Eds. D. Uhlman, N. Kreidl, Am. Ceram. Soc. Westervill, 1991.
20. T. Komatsu, V. Dimitrov, T. Tasheva, T. Honma, Electronic polarizability in silicate glasses by comparison of experimental and theoretical optical basicities, Int. J. Appl. Glass Sci., 12, 3, 2021, 424-442. https://doi.org/10.1111/ijag.16009
21. K.H. Sun, Fundamental condition of glass formation, J. Am. Ceram. Soc., 30, 1947, 277-281.
22. V. Dimitrov, T. Komatsu, Relationship between optical basicity and average single bond strength of oxide glasses, Phys. Chem. Glasses: Eur. J. Glass Sci. Technol. B, 46, 5, 2005, 521-529.